APEM journal

Advances in Production Engineering & Management
Volume 18 | Number 4 | December 2023 | pp 447–461
https://doi.org/10.14743/apem2023.4.484

ISSN 1854-6250
Journal home: apem-journal.org
Original scientific paper

IoT-based Deep Learning Neural Network (DLNN) algorithm for voltage stability control and monitoring of solar power generation

Shweta, Raj[a,*], Sivagnanam, S.[b], Kumar, K.A.[c]

[a]Annamalai University, Tamilnadu, India
[b]Annamalai University, Tamilnadu, India
[c]BHEL, Tamilnadu, India

A B S T R A C T

Today, Solar Photovoltaic (SPV) energy, an advancing and attractive clean technology with zero carbon emissions, is widely used. It is crucial to pay serious attention to the maintenance and application of Solar Power Generation (SPG) to harness it effectively. The design was more costly, and the automatic monitoring is not precise. The main objective of the work related to designed and built up the Internet of Things (IoT) platform to monitor the SPV Power Plants (SPVPP) to solve the issue. IoT platform designing and Data Analytics (DA) are the two phases of the proposed methodology. For building the IoT device in the IoT platform designing phase, diverse lower-cost sensors with higher end-to-end delivery ratio, higher network lifetime, throughput, residual energy, and better energy consumption are considered. Then, Sigfox communication technology is employed at the Low-Power Wireless Area Network (LPWAN) communication layer for lower-cost communication. Therefore, in the DA phase, the sensor monitored values are evaluated. In the analysis phase, which is the most significant part of the work, the input data are first pre-processed to avoid errors. Next, to monitor the Energy Loss (EL), the fault, and Potential Energy (PE), the solar features are extracted as of the pre-processed data. The significance of utilizing the Transformation Search centered Seagull Optimization (TSSO) algorithm, the significant features are chosen as of the extracted features. Therefore, the computational time of the solar monitoring has been decreased by the Feature Selection (FS). Next, the features are input into the Gaussian Kernelized Deep Learning Neural Network (GKDLNN) algorithm, which predicts the faults, PE, and EL. In the experimental evaluation, solar generation is assessed based on Wind Speed (WS), temperature, time, and Global Solar Radiation (GSR). The systems are satisfactory and produce more power during the time interval from 12:00 PM to 1:00 PM. The performance of the proposed method is evaluated based on performance metrics and compared with existing research techniques. When compared to these techniques, the proposed framework achieves superior results with improved precision, accuracy, F-measure, and recall.

A R T I C L E I N F O

Keywords:
Solar photovoltaic (SPV);
Internet of things (IoT);
Data analytics;
Sigfox communication technology;
Low-power wireless area network (LPWAN);
Energy loss;
Machine learning;
Transformation search centered seagull optimization algorithm (TSSO);
Gaussian kernelized deep learning Neural Network (GKDLNN)

**Corresponding author:*
shwetaraj434@gmail.com
(Shweta, R.)

Article history:
Received 3 April 2023
Revised 13 December 2023
Accepted 15 December 2023

1. Introduction

Owing to the economic and sustainable characteristics, the RE is drawing considerable attention in research [1]. Solar energy has several benefits despite more RE being available. Here, via a Photovoltaic System (PVS), electrical energy is acquired. The solar panels which can directly convert sunlight or solar energy into electricity are included in this system [2]. Temperature, irradiance, voltage, and current are the fundamental parameters that affect the solar panel's efficiency. Owing to the disparities in the temperature, solar irradiance, weather conditions, together with several other factors, the power produced from SPV installations is vulnerable [3]. Therefore, a real-time solar monitoring system is necessary for augmenting the PV panel's performance by contrasting it with the experimental outcome to start preventative action [4, 5]. The PV Monitoring System (PVMS), which is based on both wired and wireless networks, is designed to transmit parameters to a remote coordinator. This coordinator provides a web-based application for remote access [6]. Recently, the SPVMS has been incorporated with a wireless platform that involves data acquisition as of diverse sensors along with nodes via wireless data transmission [7, 8]. In the project data's practical verification and in the optimization of power plants' conversion efficacy, data acquisition is extremely significant [9-12]. The IoT facilitates objects to be recognized along with managed remotely over the prevailing system, developing new doors for the physical world's unadulterated integration into computer-centered systems and resulting in enhanced accuracy, economic benefits, together with productivity [13, 14]. For transmitting the data to the cloud, sensors and microcontrollers play an extremely vital part in relation to Wi-Fi module [14, 15-17]. Amassing data, a network layer for the data's transmission, a data processing layer for processing essential data, and finally, an application layer that operates as an interface betwixt end devices and the network all are the four-layer IoT structure in the solar-centered IoT monitoring system [18]. Wireless sensor networks, GPS, 2G/3G/4G, GPRS, GSM, WI-FI, microcontroller, RFID, microprocessor, etc. accomplish this IoT [19, 20]. On a range of parameters like energy extracted, energy potential, historical generation analysis, fault identification, and related ELs, the PVMS's intention is to offer accurate data [21]. Tracking the panel voltage, temperature, current, and the solar system's real data is to be synchronized as of time to time are the numerous difficulties faced by the solar PVS's remote monitoring [22]. There is an assortment of advantages in utilizing IoT, like enhanced accuracy, efficacy, lesser human involvement, along with cost reduction, which is exhibited by numerous investigations [23, 24]. On the monitor, the historical data and extracted energies are effortlessly presented. The manual computation takes a longer time when faults, PE, and ELs are not manually computed. Therefore, for SPVPP's DA, this work exhibits the design together with the development of an IoT platform.

2. Literature review

Kandimalla and Kishore [25] designed a prototype for the implementation of a cost-efficient technique based on IoT. This prototype checks an SPVPP for performance assessment using open-source tools and resources such as Thingspeak and Arduino. Thingspeak, a Software as a Service (SaaS) platform, provides web space for monitoring parameters. On Website designing and maintenance, Thingspeak offered every service for free of cost, which saved many investments. Thus, for the ordinary people who set up rooftop solar plants, it concentrated on a lower-cost system with a simple interface so that they could monitor the solar plants effortlessly, devoid of depending on service providers. Besides real-time monitoring, it facilitated Fault Detection (FD), preventive maintenance, along with plant's historical analysis.

Almonacid-Olleros *et al.* [26] examined the output power generation's evaluation by human-crafted characteristics with numerous temporal windows along with Deep Learning (DL) methodologies to acquire relative outcomes concerning the PV system's analytical models regarding error metrics along with learning time. In a PVS with IoT capacities created within the Opera Digital Platform underneath the Univer Project, the surrounding data along with ground truth of energy production had amassed, which was installed for two decades on the Campus of the University of Jaén (Spain). When analogized to the existing analytical model, the machine learning models provided enhanced outcomes, with considerable dissimilarities in learning time together with performance. For enriching the performance, the multiple temporal windows' utilization had exhibited as an appropriate tool to model temporal features.

Ramamurthi and Nadar [27] concentrated on an SPP's interdisciplinary field in India's southern region. It was integrated with the latest digital technology of IoT that bolstered to check real-time data of temperature, solar irradiation, panel voltage, peak power, current, together with the tilt angle of solar panels. Also, to manage the solar panel's optimum inclination angle for augmenting PV power utilizing the Genetic Algorithm (GA). For enhancing the system's tracking behaviour, an integrated SPP with IoT had constructed with hardware setup along with it was virtually tested. The performance of monitoring together with maintenance of power plant parameters with cost-efficiency had considerably improved by the IoT-centered control of SPPs [28-31].

Shapsough *et al*. [32] proffered an IoT-centered architecture, which employs IoT hardware, software, along with communication technologies to facilitate real-time monitoring together with the management of SPVMS at huge scales. This system facilitated stakeholders to remotely regulate and observe the PVSs along with to inspect the diverse environmental factor's effects like soiling, air quality, along with the weather. Regarding the network delay along with resource consumption, the system was executed and examined. For wide-ranging real-time communication, Message Queueing Telemetry Transport (MQTT) was utilized. Since the average network delay was lesser than 1 s, it was verified that the architecture was perfect for solar along with smart grid monitoring systems. The assessment exhibited that the hardware consumes about 3 % of the panel's output for resource consumption, whilst the application as well used an extremely small percentage of the CPU [33]. Since the lower-cost constrained edge devices deployed the architecture in an excellent way where the incorporation of IoT-centered paradigm, effective MQTT communication, along with lower-resources consumption made this system cost-efficient and scalable.

Pulungan *et al*. [34] explained the design, manufacture along with testing of a single axis online solar tracker monitoring system with the IoT. In real-time, the monitoring outcome's data retrieval occurred and was exhibited in the graphic data's form. Next, the data acquired as of sensors was linked to a microcontroller, and then linked to a WIFI module [8]. Samkria *et al*. [30] presented IoT along with LabVIEW-centered automatic FD of 3 × 3 solar array systems for controlling and observing internet connectivity distantly [35-36]. In the PVS, to produce a panel alert for damaged panels, the handling of the GUI indicator aided the monitoring system. Through internet connectivity, node MCU in the receiver segment facilitated fault status' transmission of PV arrays. Intended for visualizing the 3 × 3 PV array's fault status, the IoT-centered Blynk app was utilized. The Blynk's dashboard visualized each array with the status.

3. Methodology

3.1 Design and development of IOT platform for analytics of solar power

A larger percentage of the energy produced as of renewable resources is shared by the SPV, which is one of the well-known sustainable energy sources. Monitoring technologies have attained substantial focus corresponding to the performance advancement since the necessity for solar energy has increased immensely in recent decades. Presently, via wireless data transmission, the SPV-MS has been incorporated with the wireless platform, which includes data acquisition as of several sensor nodes. Nevertheless, signal interference, larger data management, security, and long-range data transmission are the challenges that influence the performance of SPV-MS. Therefore, with the DA of S-PVPP monitoring, the IoT platform has been developed here regarding various sensor devices along with varied communication technologies. IoT platform designing along with DA of SPV data was encompassed in this proposed methodology. Sensors, solar panel model, Wi-Fi module, and authentication are explicated in the IoT platform design. In DA, pre-processing, feature extraction, FS, and analysis steps are performed to assess the data. By wielding the TSSO model, the FS is conducted. Then, the GKDLNN is employed for the assessment. Fig. 1 exhibits the proposed methodology's block diagram.

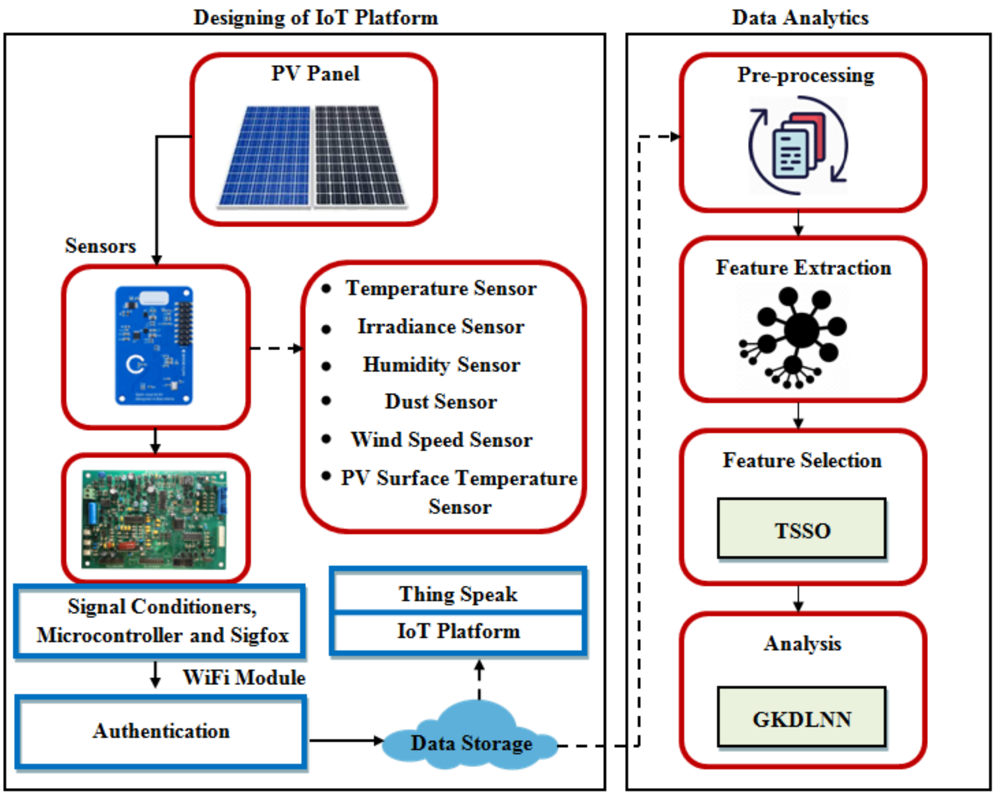

Fig. 1 A Block diagram for the proposed research methodology

3.2 Designing IoT platform

Initially, to obtain the SPV data, the IoT platform is designed. Firstly, the SPV model is structured for the design. Next, to sense the values with higher end-to-end delivery ratio, lower cost, higher network lifetime, residual energy, better energy consumption, throughput, along with better performance, the sensor of IoT devices is chosen. Then, the authentication phase is executed. The device is permitted to forward the data if it is an authorized device. The Wi-Fi module was structured to transfer the data. In this, the Sigfox technology at the LPWAN communication layer is employed for communication purposes. A greater performance was offered by the Sigfox technology at a lower cost.

3.3 Solar PV model

The sunlight is converted into DC electrical energy with a set of parallel along with series PV cells, which are included in the PV panels. At the PV modules' terminals, the observation of the characteristics desires the accumulation of extra parameters to the basic equation:

$$H = H_{PV} - H_o\left[\exp\left(\frac{L+R_sH}{\lambda L_t}\right) - 1\right] - \frac{K+R_sH}{R_p} \tag{1}$$

The PV and saturation currents are specified as H_{PV} and H_o, the diode's ideality factor is signified as λ, the series and parallels resistances are defined as R_s and R_p, and the thermal voltage is proffered as L_t. The H_{PV} is expressed as:

$$H_{PV} = \left(H_{PV,n} + M_l \Delta E\right)\frac{Q}{Q_n} \tag{2}$$

The light generated current is notated as $H_{PV,n}$, the short circuit current-temperature coefficient is proffered as M_l, the temperature difference betwixt the actual and nominal values is illustrated as E, the solar irradiation and its nominal value are described as Q and Q_n. $H_{PV,n}$ in conjunction with H_o is formulated as:

$$H_{PV,n} = \frac{R_p+R_s}{R_p}H_{sc,n} \tag{3}$$

$$H_o = \frac{H_{sc,n} + M_l \Delta E}{\exp\left(\frac{L_{oc,n} + M_v \Delta E}{\lambda L_t}\right) - 1} \tag{4}$$

The short circuit current in conjunction with open-circuit voltages underneath the nominal condition is represented as $H_{sc,n}$, $L_{oc,n}$, the open-circuit voltage per temperature coefficient is indicated as M_v. To generate the desired output power, the larger PVPP contains numerous PV modules, which are linked in series-parallel. This PVPP is modelled as:

$$H = O_p H_{PV} - O_p H_o \left[\exp\left(\frac{L + R_s\left(\frac{O_m}{O_p}\right)H}{O_m \lambda L_t}\right) - 1\right] - \frac{L + R_s\left(\frac{O_m}{O_p}\right)H}{R_p\left(\frac{O_m}{O_p}\right)} \tag{5}$$

The number of series-connected modules in a string is specified as O_m; in addition, the number of parallel-connected strings is signified as O_p. The DC-DC Buck-boost converter is wielded in the SPV module; similarly, to maximize the power, the Maximum Power Point Tracking (MPPT) is utilized.

3.4 Measurement of sensors

Various sensors are utilized to gauge the PV model's characteristics. In this, six varied sensors are considered. The solar irradiance SP110, ambient temperature DS18B20, dust GP2Y1010AU0F, humidity DHT22, WS anemometer, and the PV module surface temperature sensor PT100 are read by the six sensors. The terms in the sensor device SD are denoted as:

$$SD = \{Te, Ir, Hu, Du, Wi, St\} \tag{6}$$

The temperature sensor device is specified as Te, the irradiance device is signified as Ir, the humidity device is illustrated as Hu, the dust device is proffered as Du, the wind device is defined as Wi, and the surface temperature sensor device is symbolized as St.

Temperature sensor: The DS18B20 sensor is utilized to gauge the temperature. The DS18B20 is a 1-wire programmable Temperature sensor. With a decent accuracy of ± 5 °C, an extensive range of temperature can be measured from -55 °C to +125 °C. The values in the hard along with soft environments are gauged by this sensor.

Irradiance sensor: The SP110 sensor, which is a self-powered, analog sensor with a 0-400 mV output, is employed to measure solar irradiance. An effortless connection of dataloggers along with controllers is achieved by this sensor, which integrates a silicon-cell photodiode with a rugged, self-cleaning sensor housing design, together with a higher-quality cable terminating in a pre-tinned pigtail.

Humidity sensor: The DHT22 sensor, which is an essential, lower-cost digital temperature along with a humidity sensor, is employed for gauging the humidity. To gauge the surrounding air, a capacitive humidity together with a thermistor is utilized; subsequently, it discharges a digital signal on the data pin (analog input pins are not required). It has several benefits like having 0-100 % humidity readings with 2-5 % accuracy. In addition, it is better for -40 °C to 80 °C temperature readings with ± 0.5 °C accuracy.

Dust sensor: A simple air monitoring module with onboard Sharp GP2Y1010AU0F is termed a Dust Sensor. Fine particles, which are greater than 0.8 µm in diameter, even like cigarette smoke, are discovered by this sensor. The sensor's analog voltage output is linear with dust density. To sustain an extensive range of power supplies, an embedded voltage boost circuit has been utilized by this module.

Wind speed sensor: For utilizing this module, the black wire is linked to the power along with the signal ground, the brown wire is connected to 7-24VDC (9 V is utilized with success); in addition, the analog voltage is measured on the blue wire. The voltage ranges from 0.4 V (0 m/s wind) up to 2.0 V (for 32.4 m/s WS).

PV surface temperature sensor: The PT100 sensor is employed for gauging the PV surface temperature. Therefore, the sensor is steady, fast, along with precise. The IP65 field, which is an onsite 2-point calibration, has exceptional long-term stability.

3.5 Authentication

The sensor nodes must be registered on the server to transfer the data. The data as of the authorized sensor devices alone is received by the server. Initially, the sensor devices are registered. Details about sensor devices are provided in the registration phase. Therefore, in the database, the details are amassed. The device login to the server at the time device along with personal password is provided to transmit the data. In the verification phase, the device is permitted to broadcast the data to the server only if the details presented in the login phase are existed in the database or else the device is specified as an unauthorized device. The authentication factors are signified as:

$$Rg \rightarrow (DN, pwd, GC) \tag{7}$$

$$Ln \rightarrow (DN, pwd) \tag{8}$$

$$Vr \rightarrow \begin{cases} \text{Allowed, if } Ln = Rg \\ \text{Not allowed, otherwise} \end{cases} \tag{9}$$

The authentication's registration, verification, and verification process are notated as Rg Ln and Vr, the sensor device's device name and general characteristics are symbolized as DN and GC, and the password is exhibited as pwd.

Wi-Fi Module: Prior to amassing the computed data on an IoT server or cloud, it is processed by the AT Mega 328 (ESP8266) utilizing a Wi-Fi module. The renowned Thingspeak IoT platform is used for regular, weekly, and monthly data analysis.

Data storage: The sensed data are amassed in the cloud server with the aid of the Wi-Fi module. Petabytes of data, which are required to be amassed, processed, along with evaluated, are produced by sensor networks. In storage services, an effectual role is performed by cloud computing.

Data Analytics: The data being gathered are evaluated here. On the monitor, the energy along with historical power generation is displayed. The automatic monitoring process is desired since the prediction fault, EL, and PE are not conducted effortlessly in the manual process. The procedures in automatic DA are explicated below.

Pre-processing: Firstly, the pre-processing is performed. Some missing values along with repeated values might occur in the sensor data. An error is caused at the end of the evaluation if there occurs any missing along with repeated value in the dataset. The mean value of before together with after values of the missing place is computed to replace the missing values. The mean computation is expressed as:

$$T_i = \frac{T_{i+1} + T_{i-1}}{2} \tag{10}$$

The after value as of the missing value is represented as T_{i+1} and the before value is indicated as T_{i-1}. By employing the Hadoop-MapReduce (MR) function, the repeated data are eliminated. For writing applications, Hadoop-MR, which is a programming along with software framework, is utilized. Here, an enormous amount of data is processed speedily on larger clusters of computed nodes. Map phase and reduce phase are the two phases utilized here. Every single phase contains key-value pairs as input as well as output. Regarding the data structured (key, value) in pairs, the map along with reduce functions of MR are proffered. A set of input key-value pairs is taken during computation; thus, producing a set of output key-value pairs. The map along with reduce functions in Hadoop-MR is formulated as:

$$M_p(\alpha_1, T_1) \rightarrow l_t(\alpha_2, T_2) \tag{11}$$

$$C_e\big(\alpha_2, l_t(T_2)\big) \rightarrow l_t(T_2) \tag{12}$$

The map function is specified as M_p, the key values are signified as α_1 and α_2, the reduce function is defined as C_e and the list of MR functions is proffered as l_t.

3.6 Feature extraction

Subsequent to pre-processing, from the pre-processed data, the features are extracted. Relative Humidity, Irradiance, Temperature, PV surface Temperature, WS, and Dust Accumulation are the features being extracted. The feature terms are notated as:

$$Z_s = \{z_1, z_2, z_3, \ldots., z_n\}, \text{or } z_i, i = 1,2, \ldots., n \tag{13}$$

The feature set is indicated as Z_s and the n-number of features is depicted as z_n.

3.7 Feature selection

Here, to alleviate the monitoring process's computational time, as of the feature set being extracted, the significant features are chosen. The TSSO algorithm is deployed in the proposed model. The migration along with the behaviours of seagulls in nature is inspired for the development of the Seagull Optimization (SO) algorithm. Seagulls are a type of seabird. They encompass various species that primarily feed on fish, insects, amphibians, reptiles, and earthworms. This version is more direct and clearer. They are extremely intelligent and use their intelligence to find food and attack prey. For instance, they use breadcrumbs to attract fish, and to catch earthworms hidden underground, they mimic the sound of rain with their feet. A better performance was offered by the traditional SO algorithms. However, the issue of poor exploration along with exploitation searching capacity is faced them. Thus, in this paper, the transformation search is applied in the SO algorithm to address the aforementioned problem. The most crucial behaviours of seagulls are migration along with attack. The source food for seagulls is proffered as migration behaviours. The seagulls' attack towards the migrating birds at sea is mentioned as attack behaviour. Firstly, the populations are initialized. In this, the features being selected are regarded as the population. By the transformation search function, the population is initialized. It is represented as:

$$A_i = \varpi(lb + ub) - (z_i - \tilde{z}_i) \tag{14}$$

The initialized population set is proffered as A_i, the elastic factor is notated as ϖ, the upper and lower bound values are denoted as lb and ub. Next, the Fitness Value (FV) is computed. In this, the accurate evaluation is pondered as a FV. Following initialization, the migration along with the attacking behaviours is explicated individually.

(a) Migration behaviour

The algorithm imitates the seagulls' movement from one place to another during the migration process. Avoiding collisions, the best position's direction, and reaching the best position are the three criteria that must be satisfied by the seagulls. These criteria are explicated as follows. Initially, an extra variable F is presented to avoid collisions. Thus, betwixt the neighbours, the collision is prevented. For the new Search Agent (SA) position, the new variable is utilized.

$$LO_s = F\, W_s(t) \tag{15}$$

The SA's location that doesn't collide with other SAs is specified as LO_s, the SA's current location is indicated as W_s, the current iteration time is denoted as t, and the SA's mobile behaviour in the provided search space is signified as F.

$$F = \zeta_c - \left(t \left(\frac{\zeta_c}{ax_{it}}\right)\right), t = 0,1,2, \ldots., ax_{ite} \tag{16}$$

To regulate the utilization frequency of variable F, the parameter ζ_c is introduced. The variable F is linearly reduced from ζ_c to 0. After satisfying the condition of not colliding with other individuals, the seagull moves towards the best position. It is illustrated as:

$$SA_s = \delta \left(W_{bs}(t) - W_s(t)\right) \tag{17}$$

The position of current location Search Agent is indicated $SA\ W_s$ towards the best-fit $SA\ W_b$ (that is to say, the best seagull with a smaller FV) is represented as SA_s. The behaviour of δ, which is accountable for appropriate balancing betwixt exploration and exploitation, is randomized. It is gauged as:

$$\delta = 2\,F^2\,r \tag{18}$$

A random number which lies in the range of [0, 1] is specified as r. Finally, regarding the best SA, the SA can update its position.

$$\varphi_s = |LO_s + SA_s| \tag{19}$$

The distance between the SA and best-fit SA (that is to say, best seagull whose FV is less) is denoted as φ_s.

(b) Attack behaviour

The seagulls make a spiral motion in the air whilst attacking the prey. This behaviours in u, v, and x planes are elucidated as:

$$u' = d\cos(y) \tag{20}$$

$$v' = d\sin(y) \tag{21}$$

$$x' = d\,y \tag{22}$$

$$d = p\,e^{yq} \tag{23}$$

The radius of every single turn of the spiral is specified as d, a random number in the range $[0 \le y \le 2\pi]$ is defined as y, constants to proffer the spiral shape are notated as p and q, and the natural logarithm's base is represented as e. The SA's updated position is computed by wielding the Eqs. 15-23.

$$W_s(t) = \left(\varphi_s\,u'\,v'\,x'\right) + W_{bs}(t) \tag{24}$$

The best solution is saved together with the position of other SAs is updated by the $W_s(t)$.

```
Input: Extracted features z_i
Output: Selected features z̃_i
Begin
    Initialize population A_i, iteration t, and maximum iteration ax_it
    Set t = 1
    While (t ≤ ax_it) do
        Calculate Fitness function
        //Migration Behaviour//
        r = rand(0,1)            /* To generate the random number in range [0, 1] */
        y = rand(0,2π)           /* To generate the random number in range [0, 2π] */
        //Attacking Behaviour//
        d = p × e^yq             /* To generate the spiral behavior during migration */
        Calculate distance φ_s
        W_s(t) = (φ_s × u' × v' × x') + W_bs(t)
        Set t = t + 1
    End while
    Return optimal features z̃_i
End
```

Fig. 2 Pseudo code for TSSO

Fig. 2 depicts the TSSO's pseudo-code. Fig. 3 displays the flowchart for the TSSO.

The features being selected are modelled as:

$$\tilde{Z}_s = \{\tilde{z}_1, \tilde{z}_2, \tilde{z}_3, \ldots\ldots, \tilde{z}_n\}, \text{or } \tilde{z}_i, i = 1,2,\ldots\ldots, n \tag{25}$$

The feature set is notated as $\tilde{Z}_s$ and the n-number of features is symbolized as $\tilde{z}_n$.

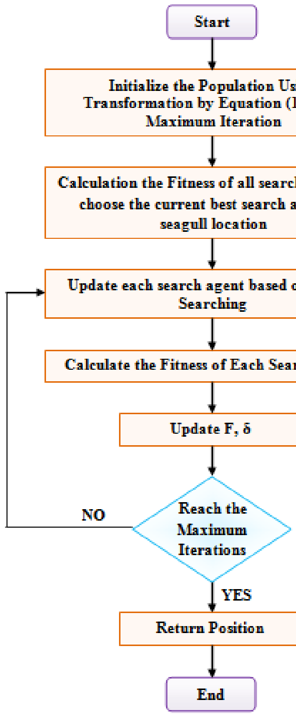

Fig 3 Flowchart for TSSO algorithm

3.8 DLLN analysis

Subsequent to FS, the features being selected are inputted to the analysis phase. Faults, PE, and EL are forecasted by this evaluation. In numerous applications, the Artificial Neural Network (ANN), which is an intelligent system, is utilized to address complex issues. Three layers are encompassed in the ANN structure. They are: (i) an Input Layer (IL), which includes the collected data, (ii) an Output Layer (OL), which generates computed data, along with (iii) one or more Hidden Layers (HLs), which are apt for linking the IL along with the OL. Collecting input and generating output are the two functions performed by a neuron, which is a fundamental processing unit of a NN. To obtain an output, every single input is multiplied by connection weights; the products and biases are added. Afterwards, they are passed via an Activation Function (AF). However, for the deep analysis, a single HL is possessed by the traditional NN. A more number of HLs is utilized in this proposed framework. A random weight initialization methodology is possessed by the baseline algorithm. In the output, a minor alteration in weight initialization can lead to a critical change, thereby worsening the outcome. Regarding the Gaussian neighbourhood function, the weight values are altered in the proposed methodology to conquer the aforementioned complication. Additionally, an effective AF is desired for the deep analysis. Consequently, the kernelized AF is utilized here. With this alteration, the NN is renamed as the GKDLNN algorithm. Fig. 4 displays the GKDLNN's structure.

To start with, the selected features $\tilde{z}_i$ are inputted to the IL. Subsequently, the HL is provided with the IL's output. Regarding the weights, which is the sum of weighted synapse connections, the output is computed by the HL. The input is filtered by eliminating the redundant data and is forwarded to the subsequent HL for further processing. The HL process is mathematically formulated as:

$$hd_i = ib_s + \sum_{i=1}^{n} \tilde{z}_i . \varepsilon_i \tag{26}$$

Here, the bias value is notated as ib_s, the weight value is symbolized as ε_i, and the input feature is signified as $\tilde{z}_i$. By employing the Gaussian neighbourhood function, the weight adjustment is derived as:

$$\varepsilon_{i+1} = \varepsilon_i + NN_i[\tilde{z}_i - \varepsilon_i] \tag{27}$$

The Gaussian neighbourhood function is modelled as NN_i.

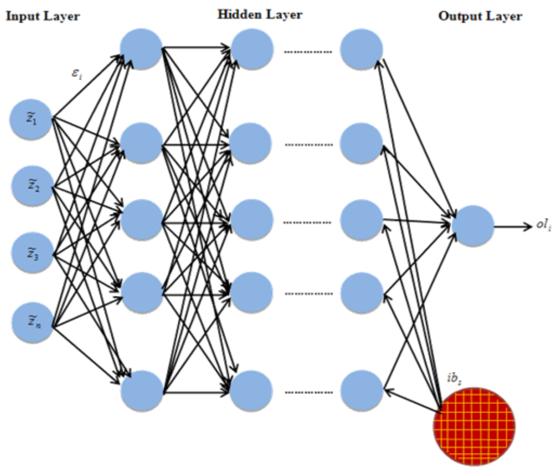

Fig. 4 Structure of the DLNN algorithm

$$NN_i = \tau_i \, e^{\left(-\frac{\|cp_c - cp_p\|^2}{2\sigma_i^2}\right)} \tag{28}$$

The learning rate is exhibited as τ_i, the coordinate positions of the current neuron and the previous neuron are depicted as $cp_c$and cp_p, and the neighbourhood radius's width is proffered as σ_i. Consequently, the HL output is inputted to the OL, in which by pondering the kernelized function, the AF is obtained as:

$$ol_i = ib_s + \sum_{i=1}^{n} \gamma_i \, (hd_i \, \varepsilon_i) \tag{29}$$

Herein, the output unit is specified as ol_i and the kernelized function is signified as γ_i. Finally, the loss function is measured as:

$$ls = (ta - ol_i) \tag{30}$$

The loss function is exhibited as ls, the output unit is illustrated as ol_i and the network's target output is depicted as ta. The obtained loss is verified whether it is matched with the specified threshold value or not. If it is matched, then the output is mentioned as the final output or else the weight value is altered again.

4. Result and discussion

Here, the proposed research technique's performance is examined. MATLAB has been employed to execute the IoT platform design and SPVPP DA. The proposed model utilizes publicly obtainable data for the performance investigation.

4.1 Performance analysis of displayed values

The sensed values as of the sensor are examined here. Regarding temperature, time, GSR, along with WS, the SPG is evaluated.

Regarding diverse time instants, Fig. 5 exhibits the SPG. From 6:00 to 19:00, it can perceive. For SPP monitoring, it is one of the other vital parameters. The solar generation level is higher at 12:00 and 13:00. The SPG is lesser for the remaining time. Regarding the temperature variation, Fig. 6 presents the SPG. It is noticed that as the temperature increases, the SPG also increases. The generated solar power is 3500 kW if the temperature is 270 °C. The solar power is 1725 kW if the temperature is 25.50 °C. Therefore, it exhibits that the temperature change offers a large effect on SPG.

Regarding WS changes, Fig. 7 displays the SPG. For power plant monitoring, it is a significant parameter. For the WS's variation, the vast difference is not exhibited. SPG is varied slightly. However, the higher SPG is acquired for the WS of 16.3 km/h. Fig. 8 exhibits the SPG regarding GSR. It is observed that the SPG is increased as the average GSR is increased. The generated solar power is 3900 kW when the average GSR is 5. Conversely, the solar power generated is 995 kW when the average GSR is 1.5. Hence, on SPG, there is a larger effect of average GSR.

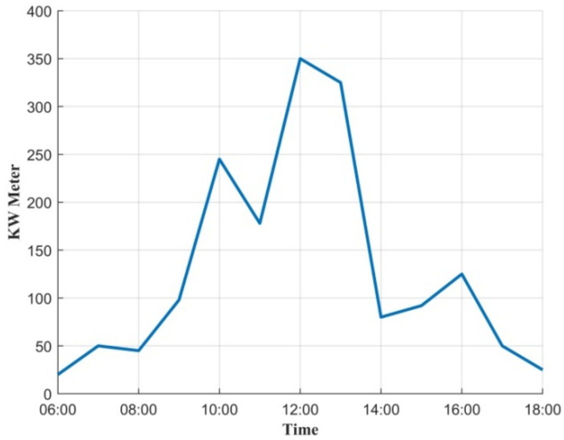

Fig. 5 Analysis of SPG at different time instants

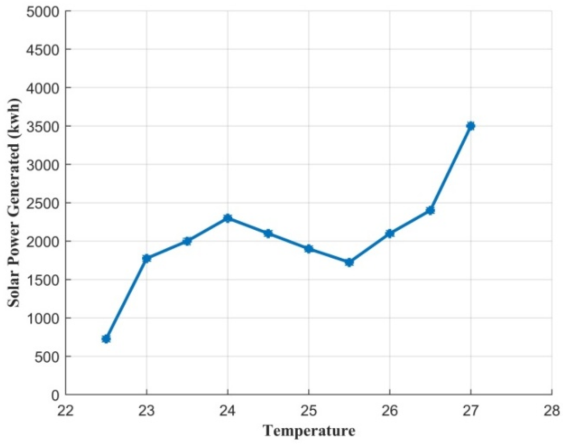

Fig. 6 Analysis of SPG with respect to temperature

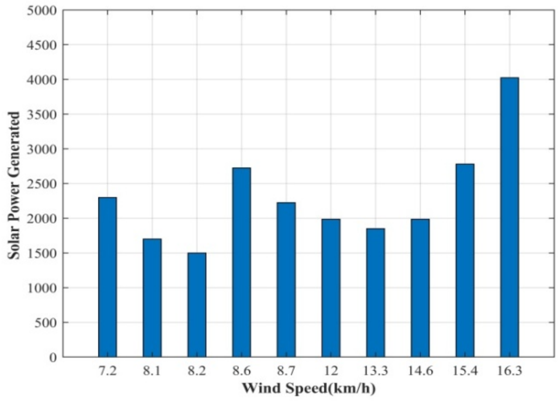

Fig. 7 Analysis of SPG with respect to WS

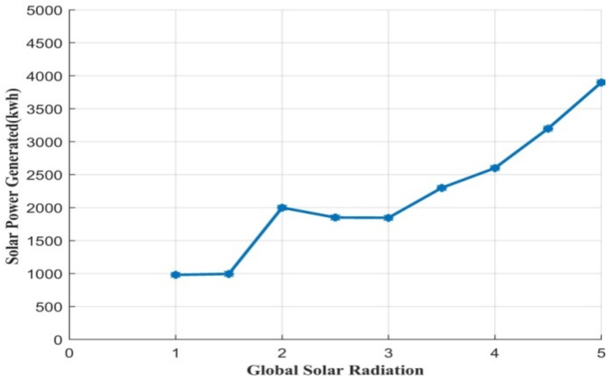

Fig. 8 Power generation analysis with respect to the global solar radiation changes

4.2 Performance analysis of solar power plant monitoring

Here, regarding precision, accuracy, F-measure, and recall metrics, the performance of the SPP monitoring by the GKDLNN is evaluated with the prevailing Support Vector Machine (SVM), ANN, Convolutional NN (CNN), and DLNN algorithms. Furthermore, regarding fitness vs. iteration analysis, the TSSO centered FS process's performance is analogized with prevailing GA, Particle Swarm Optimization (PSO), Gray Wolf Optimization (GWO), and SO.

Regarding precision, accuracy, F-measure, and recall metrics, the GKDLNN centered SPP monitoring along with the prevailing algorithm-centered monitoring system's performance is exhibited in Table 1. When analogized to the other prevailing algorithms and the GKDLNN algorithm, the prevailing SVM acquires extremely poor performance in this investigation. On considering the prevailing method, the GKDLNN algorithm acquires higher-level performance. Here, the prevailing DLNN surpassed the other prevailing algorithms; however, it is also lesser than the GKDLNN algorithm.

Table 1 Performance analysis of proposed GKDLNN with the existing algorithm based on performance metrics

Performance Metrics	Proposed GKDLNN	DLNN	CNN	ANN	SVM
Accuracy	96.5	91	88	83.2	79
Precision	94	89.3	85	81.3	78
Recall	94.5	90.3	86	81.5	79.2
F-Measure	94.24	89.79	85.49	81.39	78.59

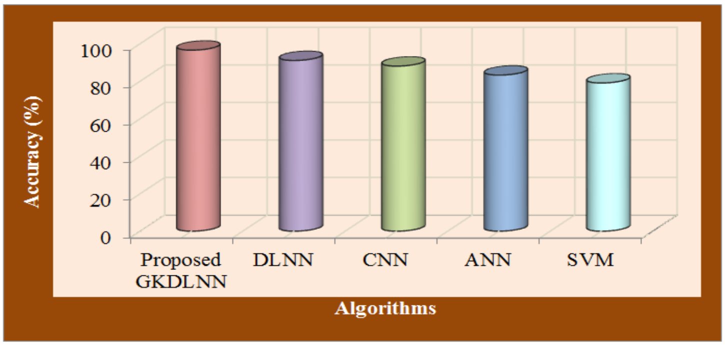

Fig. 9 Graphical representation of accuracy analysis for the proposed and existing algorithms

In Fig. 9, the pictorial depiction of accuracy investigation for the GKDLNN centered SPP monitoring is analogized with the prevailing algorithm-centered monitoring like SVM, ANN, CNN, and DLNN algorithms. The common assessment metric for the predictions is the accuracy metric. It is the number of correct predictions made as a ratio of every prediction done. Accuracy of 96.5 % is acquired by the GKDLNN methodology, which is higher than the prevailing study techniques. For DLNN, CNN, ANN, and SVM, the prevailing technique's accuracy values are 91 %, 88 %, 83.2 %, and 79 %, respectively.

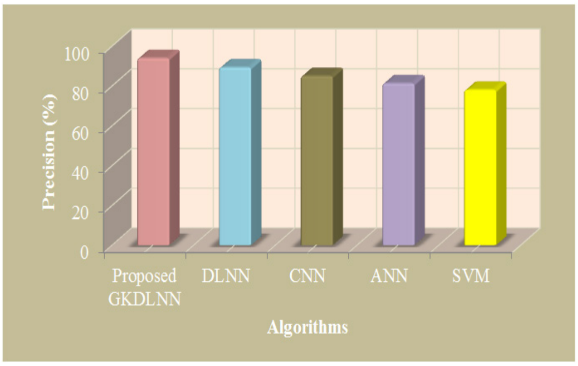

(a)

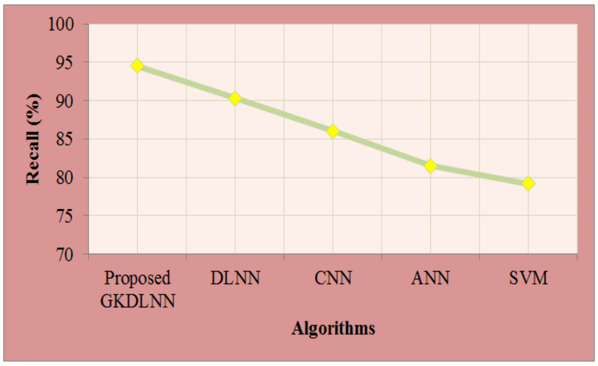

(b)

Fig. 10 Demonstrate the performance of the proposed and existing algorithms in terms of (a) precision and (b) recall metrics

Regarding (a) precision and (b) recall metrics, the GKDLNN method's performance investigation with the prevailing algorithms is displayed in Fig. 10. The two very vital model evaluation metrics are recall and precision. Precision implies the percentage of the outcomes which is pertinent, recall implies the percentage of total pertinent outcomes precisely classified by the algorithm. The GKDLNN algorithm accomplished 94 % of precision and 94.5 % of recall; however, the prevailing algorithms like DLNN, CNN, ANN, and SVM have 89.3 % and 90.3 %, 85 % and 86 %, 81.3 %, and 81.5 %, and 78 % and 79.2 %, respectively. When analogized to the prevailing study techniques, the GKDLNN accomplishes higher performance in this analysis.

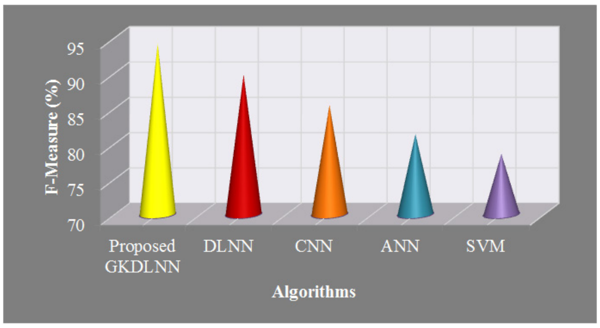

Fig. 11 F-Measure analysis

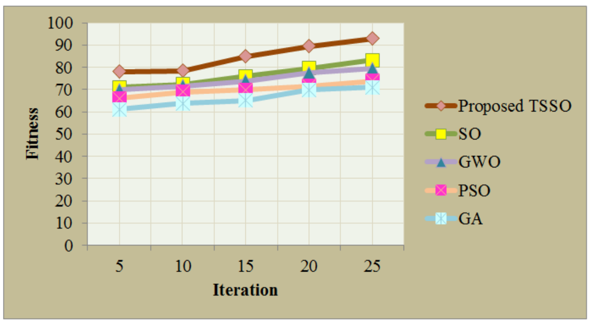

Fig. 12 Fitness vs. iteration analysis

The GKDLNN and prevailing technique's F-measure are exhibited in Fig. 11. F-Measure is the harmonic mean value of the precision and the recall metric. A higher value is also accomplished by the F-measure. The GKDLNN method accomplishes better performance centered on the precision together with recall metrics, so the F-measure-centered analysis is better for the GKDLNN method. Here, an F-measure of 94.24 % is acquired by the GKDLNN technique. The prevailing algorithms' F-measures are 89.79 % for DLNN, 85.49 % for CNN, 81.39 % for ANN, and 78.59 % for SVM. Therefore, the GKDLNN technique's performance surpassed the prevailing techniques as per the analysis.

The TSSO algorithm's fitness vs. iteration investigation with the prevailing GWO, GA, SO, and PSO algorithms are displayed in Fig. 12. The TSSO algorithm's FV is 85 when the iteration count is 15; however, the prevailing techniques namely SO, GWO, PSO, and GA have 76, 73.89, 69.9, and 65.1, respectively. When analogized to the prevailing technique, the TSSO has a greater fitness value for the other iterations also.

5. Conclusion

In this work DA of SPVPPs, an IoT platform's design and development are presented. IoT design and DA are the two phases of this study method. The LPWAN communication layer is employed with Sigfox communication technology, and diverse sensors are employed in the IoT designing phase. The PE, EL, and the fault are evaluated in the DA phase. The GKDLNN algorithm is primarily utilized for analytics. The publicly obtainable dataset is wielded for the performance study. In the outcome analysis phase, the sensed values as of the sensor are plotted, and regarding the recall, precision, F-measure, and accuracy, the GKDLNN algorithm's performance is verified with the prevailing DNN, ANN, DLNN, and SVM models. The GKDLNN methodology acquires the greatest accuracy of 96.5 %. Furthermore, regarding fitness, the TSSO's performance is scrutinized with the prevailing GA, PSO, GWO, and SO. Better performance is achieved by the TSSO algorithm. Therefore, for the SPVPP monitoring, the recommended technique-centered monitoring and the chosen devices are highly cooperative. For ameliorating the system's performance, the proposed mechanism can be expanded encompassing more sensors, the latest devices, along with advanced algorithms.

References

[1] Shakya, S. (2021). A self monitoring and analyzing system for solar power station using IoT and data mining algorithms, *Journal of Soft Computing Paradigm,* Vol. 3, No. 2, 96-109, doi: 10.36548/jscp.2021.2.004.

[2] Priharti, W., Rosmawati, A.F.K., Wibawa, I.P.D. (2019). IoT based photovoltaic monitoring system application, *Journal of Physics: Conference Series,* Vol. 1367, Article No. 012069, doi: 10.1088/1742-6596/1367/1/012069.

[3] Kekre, A., Gawre, S.K. (2017). Solar photovoltaic remote monitoring system using IOT, In: *Proceedings of 2017 International Conference on Recent Innovations in Signal processing and Embedded Systems (RISE),* Bhopal, India, 619-623, doi: 10.1109/RISE.2017.8378227.

[4] Sathesh, M., Mohana, J. (2020). IoT based monitoring and load sharing of grid connected solar PV system, *Journal of Critical Reviews,* Vol. 7, No. 6, 2223-2232, doi: 10.31838/jcr.07.6.346.

[5] Madhubala, S., Nachammai, R., Nandhini, I., Preethisha, A.M., Janet Paulin, J. (2018). Solar power based remote monitoring and control of industrial parameters using IoT, *International Research Journal of Engineering and Technology,* Vol. 5, No. 3, 3231-3236.

[6] Kavitha, V., Malathi, V. (2019). A smart solar PV monitoring system using IOT, In: *Proceedings of SRAIC 2019: First International Conference on Secure Reconfigurable Architectures and Intelligent Computing,* Tiruchirappalli Trichy, India, 1-33, doi: 10.5121/csit.2019.91502.

[7] Ansari, S., Ayob, A., Hossain Lipu, M.S., Saad, M.H.M., Hussain, A. (2021). A review of monitoring technologies for solar PV systems using data processing modules and transmission protocols: Progress, challenges and prospects, *Sustainability,* Vol. 13, No. 15, Article No. 8120, doi: 10.3390/su13158120.

[8] Babu, V., Ahmed, K.S., Shuaib, Y.M., Mani, M. (2021). A novel intrinsic space vector transformation based solar fed dynamic voltage restorer for power quality improvement in distribution system, *Journal of Ambient Intelligence and Humanized Computing,* Vol. 12, No. 1, 897-919, doi: 10.1007/s12652-020-02831-0.

[9] Pereira, R.I.S., Jucá, S.C.S., Carvalho, P.C.M. (2019). IoT embedded systems network and sensors signal conditioning applied to decentralized photovoltaic plants, *Measurement,* Vol. 142, 195-212, doi: 10.1016/j.measurement.2019.04.085.

[10] Adhya, S., Saha, D., Das, A., Jana, J., Saha, H. (2016). An IoT based smart solar photovoltaic remote monitoring and control unit, In: *Proceedings of 2nd International Conference on Control, Instrumentation, Energy and Communication (CIEC),* Kolkata, India, 432-436, doi: 10.1109/CIEC.2016.7513793.

[11] Badave, P.M., Karthikeyan, B., Badave, S.M, Mahajan, S.B, Sanjeevikumar, P., Gill, G.S. (2018). Health monitoring system of solar photovoltaic panel: An Internet of Things application, In: SenGupta, S., Zobaa, A., Sherpa, K., Bhoi, A. (eds.), *Advances in smart grid and renewable energy. Lecture notes in electrical engineering, Vol 435,* Springer, Singapore, 347-355, doi: 10.1007/978-981-10-4286-7_34.

[12] Shrihariprasath, B., Rathinasabapathy, V. (2016). A smart IoT system for monitoring solar PV power conditioning unit, In: *Proceedings of 2016 World Conference on Futuristic Trends in Research and Innovation for Social Welfare (Startup Conclave),* Coimbatore, India, 1-5, doi: 10.1109/STARTUP.2016.7583930.

[13] Ammar, M., Russello, G., Crispo, B. (2018). Internet of Things: A survey on the security of IoT frameworks, *Journal of Information Security and Applications,* Vol. 38, 8-27, doi: 10.1016/j.jisa.2017.11.002.

[14] Karbhari, G.V., Nema, P. (2020). IoT & machine learning paradigm for next generation solar power plant monitoring system, *International Journal of Advanced Science and Technology,* Vol. 29, No. 3, 7287-7295.

[15] Babu, V., Basha, S.S., Shuaib, Y.M., Manikandan, M., Enayathali, S.S. (2019). A novel integration of solar fed dynamic voltage restorer for compensating sag and swell voltage in distribution system using enhanced space vector pulse width modulation (ESVPWM), *Universal Journal of Electrical and Electronic Engineering,* Vol. 6, No. 5, 329-350, doi: 10.13189/ujeee.2019.060504.

[16] Manikandan, M., Basha, A.M. (2016). ODFF: Optimized dual fuzzy flow controller based voltage sag compensation for SMES-based DVR in power quality applications, *Circuits and Systems,* Vol. 7, No. 10, 2959-2974, doi: 10.4236/cs.2016.710254.

[17] Praveen Kumar, T., Ganapathy, S., Manikandan, M. (2022). Improvement of voltage stability for grid connected solar photovoltaic systems using static synchronous compensator with recurrent neural network, *Electrical Engineering & Electromechanics,* No. 2, 69-77, doi: 10.20998/2074-272X.2022.2.10.

[18] Ansari, S., Ayob, A., Hossain Lipu, M.S., Saad, M.H.M., Hussain, A (2020). Comparison of the IoT based modules for solar PV environment: A review, In: *Proceedings of 2020 IEEE Student Conference on Research and Development (SCOReD),* Batu Pahat, Malaysia, 401-405, doi: 10.1109/SCOReD50371.2020.9250946.

[19] Tellawar, M., Chamat, N. (2019). An exclusive review on IoT based solar photovoltaic remote monitoring and controlling unit, *International Research Journal of Engineering and Technology (IRJET),* Vol. 6, No. 5, 1520-1525.

[20] Karbhari, G.V., Nema, P. (2019). Digital control system for solar power plant using IoT, *International Journal of Recent Technology and Engineering (IJRTE),* Vol. 8, No. 2, 3394-3396, doi: 10.35940/ijrte.A1181.078219.

[21] Sutikno, T., Purnama, H.S., Pamungkas, A., Fadlil, A., Alsofyani, I.M., Jopri, M.H. (2021). Internet of things-based photovoltaics parameter monitoring system using NodeMCU ESP8266, *International Journal of Electrical and Computer Engineering (IJECE),* Vol. 11, No. 6, 5578-5587, doi: 10.11591/ijece.v11i6.pp5578-5587.

[22] Sarswat, S., Yadav, I., Maurya, S.K. (2019). Real time monitoring of solar PV parameter using IoT, *International Journal of Innovative Technology and Exploring Engineering (IJITEE),* Vol. 9, No. 1S, 267-271, doi: 10.35940/ijitee.A1054.1191S19.

[23] Gupta, V., Sharma, M., Pachauri, R.K., Babu, K.N.D. (2020). A low-cost real-time IOT enabled data acquisition system for monitoring of PV system, *Energy Sources, Part A: Recovery, Utilization, and Environmental Effects,* Vol. 43, No. 20, 2529-2543, doi: 10.1080/15567036.2020.1844351.

[24] Sathish, C., Chidambram, I.A., Manikandan, M. (2022). Reactive power compensation in a hybrid renewable energy system through fuzzy based boost converter, *Problemele Energeticii Regionale,* No. 53, 10-26, doi: 10.52254/1857-0070.2022.1-53.02.

[25] Kandimalla, J., Kishore, D.R. (2017). Web based monitoring of solar power plant using open source IOT platform Thingspeak and Arduino, *International Journal for Modern Trends in Science and Technology,* Vol. 3, No. 4, 16-21.

[26] Almonacid-Olleros, G., Almonacid, G., Fernandez-Carrasco, J.I., Espinilla-Estevez, M., Medina-Quero, J. (2020). A new architecture based on IoT and machine learning paradigms in photovoltaic systems to nowcast output energy, *Sensors,* Vol. 20, No. 15, Article No. 4224, doi: 10.3390/s20154224.

[27] Ramamurthi, P.V., Nadar, E.R.S. (2022). IoT-based energy monitoring and controlling of an optimum inclination angle of the solar panels, *IETE Journal of Research,* Vol. 68, No. 4, 3108-3118, doi: 10.1080/03772063.2020.1754301.

[28] Paredes-Parra, J.M., García-Sanchez, A.J., Mateo-Aroca, A., Molina-Garcia, Á. (2019). An alternative Internet-of-Things solution based on LoRa for PV power plants data monitoring and management, *Energies,* Vol. 12, No. 5, Article No. 881, doi: 10.3390/en12050881.

[29] Cheddadi, Y., Cheddadi, H., Cheddadi, F., Errahimi, F., Es-sbai, N. (2020). Design and implementation of an intelligent low-cost IoT solution for energy monitoring of photovoltaic stations, *SN Applied Sciences,* Vol. 2, No. 7, Article No. 1165, doi: 10.1007/s42452-020-2997-4.

[30] Samkria, R., Abd-Elnaby, M., Singh, R., Gehlot, A., Rashid, M., Aly, M.H., El-Shafai, W. (2021). Automatic PV grid fault detection system with IoT and LabVIEW as data logger, *Computers, Materials and Continua,* Vol. 69, No. 2, 1709-1723, doi: 10.32604/cmc.2021.018525.

[31] Oukennou, A., Berrar, A., Belbhar, I., El Hamri, N. (2019). Low cost IoT system for solar panel power monitoring, In: *Colloque sur les Objets et systèmes Connectés, Ecole Supérieure de Technologie de Casablanca, Institut Universitaire de Technologie d'Aix-Marseille,* Casablanca, Morocco.

[32] Shapsough, S., Takrouri, M., Dhaouadi, R., Zualkernan, I.A. (2021). Using IoT and smart monitoring devices to optimize the efficiency of large-scale distributed solar farms, *Wireless Networks,* Vol. 27, 4313-4329, doi: 10.1007/s11276-018-01918-z.

[33] Babu, V., Ahmed, K.S., Shuaib, Y.M., Manikandan, M. (2021). Power quality enhancement using dynamic voltage restorer (DVR)-based predictive space vector transformation (PSVT) with proportional resonant (PR)-controller, *IEEE Access,* Vol. 9, 155380-155392, doi: 10.1109/ACCESS.2021.3129096.

[34] Pulungan, A.B., Risfendra, R., Purwanto, W., Maksum, H., Setiawan, O. (2020). Design and development of real time monitoring single axis solar tracker by using internet of things, *International Journal of Geomate,* Vol. 18, No. 69, 81-87, doi: 10.21660/2020.69.25863.

[35] Reddy, S.G., Ganapathy, S., Manikandan, M. (2022). Three phase four switch inverter based DVR for power quality improvement with optimized CSA approach, *IEEE Access,* Vol. 10, 72263-72278, doi: 10.1109/ACCESS.2022.3188629.

[36] Reddy, S.G., Ganapathy, S., Manikandan, M. (2022). Power quality improvement in distribution system based on dynamic voltage restorer using PI tuned fuzzy logic controller, *Electrical Engineering & Electromechanics,* No. 1, 44-50, doi: 10.20998/2074-272X.2022.1.06.